Supplementary Information

From Atom to Device: An Integrated Se Cathode with Atomic Co Sites and Dual Carbon Confinement for Ultrafast Li–Se Batteries

Wen Yan,[#a] Yimin Yang, [#a] Zhangchi Xu,[a] Qingqing Wang,[a] Ying Wang,*[a] Qiyan Dai,[a] and Lei Zhang*[b]

[a]School of Chemistry and Materials Science, Jiangsu Normal University, Xuzhou, Jiangsu, 221116, P. R. China.

[b]Centre for Catalysis and Clean Energy, Gold, Coast Campus, Griffith University, Gold Coast, QLD 4222, Australia

*Correspondence: yingwang@jsnu.edu.cn, lei.zhang@griffith.edu.au

1、Experimental Section

Materials: All chemicals and reagents were used as received without further purification unless otherwise specified, including methanol (99%), polyacrylonitrile (PAN, M_w = 150,000), zinc nitrate hexahydrate ($Zn(NO_3)_2·6H_2O$), cobalt nitrate hexahydrate ($Co(NO_3)_2·6H_2O$), 2-methylimidazole, and selenium powder (99.99%).

Synthesis of ZnCo-ZIFs: $Zn(NO_3)_2·6H_2O$ (2.48 g) and $Co(NO_3)_2·6H_2O$ (0.124 g), corresponding to a Zn^{2+}/Co^{2+} molar ratio of 20, were dissolved in 100 mL of methanol under stirring for 0.5 h. Subsequently, 100 mL of methanol containing 2-methylimidazole (4.365 g) was added to the above solution, and the mixture was stirred for 24 h. The resulting precipitate (denoted as ZnCo-ZIFs) was collected by centrifugation, washed three times with methanol, and dried at 60 °C overnight.

Synthesis of ZnCo-ZIFs@PAN film: ZnCo-ZIFs powder (0.6 g) was dispersed in 7 mL of N, N-dimethylformamide (DMF) and sonicated for 90 min. PAN (0.8 g, M_w = 150,000) was then added, followed by magnetic stirring at 65 °C for 4 h and additional stirring at room temperature for 12 h to obtain a homogeneous electrospinning precursor solution. The solution was loaded into a 5 mL syringe and electrospun at a flow rate of 15 μL min^{-1} under an applied voltage of 16 kV (DW-P503-1ACH1), with a collection distance of 15 cm. The resulting nonwoven film had an area of approximately 30 × 20 cm^2.

Synthesis of Co-NC@CNFs film: The as-prepared ZnCo-ZIFs@PAN film was first stabilized in air at 260 °C for 1 h and then carbonized at 800 °C for 3 h under an inert

atmosphere with a heating rate of 5 °C min^{-1}, yielding ZnCo-NC@CNFs. The obtained film was then immersed in 2 M HCl for 12 h to remove Zn species, thoroughly washed with deionized water, and dried at 70 °C for 12 h to obtain the final freestanding Co-NC@CNFs film.

Preparation of Se/Co-NC@CNFs film: Selenium powder was loaded into the Co-NC@CNFs host through a melt-diffusion process. Specifically, Se and Co-NC@CNFs were mixed at a mass ratio of 2:1, placed in a tube furnace under Ar flow, heated to 260 °C at a rate of 5 °C min^{-1}, and maintained at this temperature for 12 h. The resulting integrated freestanding cathode was denoted as Se/Co-NC@CNFs.

Preparation of high-loading Se73/Co-NC@CNFs: For the high-Se-loading sample, Co-NC@CNFs and Se powder were mixed at a mass ratio of 1:3, sealed in an Ar-filled reactor, and heated at 260 °C for 12 h to allow sufficient selenium melt diffusion into the carbon host. The resulting sample contained 73 wt% Se and was denoted as Se_{73}/Co-NC@CNFs.

Preparation of Se/NC: For comparison, a control sample without cobalt incorporation, dual-carbon confinement, or freestanding architecture (denoted as Se/NC) was prepared. Specifically, Zn-ZIFs were synthesized following a procedure similar to that for ZnCo-ZIFs, except that only $Zn(NO_3)_2 \cdot 6H_2O$ (2.604 g) was used as the metal source without adding cobalt salt. The obtained Zn-ZIFs were subjected to the same stabilization, carbonization, and acid-etching procedures as described above to obtain a nitrogen-doped carbon matrix, denoted as NC. Selenium was then introduced into the

NC host by the same melt-diffusion method (260 °C for 12 h under Ar) at a Se/host mass ratio of 2:1, yielding the control composite Se/NC.

Preparation of Se/NC@CNFs: Another control sample without atomically dispersed Co sites (denoted as Se/NC@CNFs) was also prepared. The synthesis procedure was identical to that of Se/Co-NC@CNFs, except that only Zn-ZIFs were used in the electrospinning precursor without introducing any cobalt source. All subsequent steps, including carbonization, acid etching, and selenium melt diffusion, were carried out under the same conditions as those used for Se/Co-NC@CNFs.

Material Characterizations: X-ray diffraction (XRD) patterns were recorded on a Rigaku D/Max-2500 diffractometer using Cu Kα radiation. The morphology and microstructure were characterized by field-emission scanning electron microscopy (FESEM, JEOL SU8010), transmission electron microscopy (TEM), and high-resolution TEM (HR-TEM, Tecnai G2 F20). Thermogravimetric analysis (TGA) was performed on a TA-Q50 instrument under N_2 flow from 25 to 800 °C at a heating rate of 10 °C min^{-1} to determine the selenium content. X-ray photoelectron spectroscopy (XPS) was carried out on a Thermo ESCALAB 250XI system. Nitrogen adsorption–desorption isotherms were measured using a Quantachrome Autosorb-IQ2-VP analyzer. Raman spectra were collected on a Renishaw inVia spectrometer with a 532 nm excitation laser. The content and coordination environment of single-atom cobalt were analyzed by inductively coupled plasma optical emission spectroscopy (ICP-OES, Agilent 7850, USA), aberration-corrected transmission electron microscopy (AC-TEM, JEOL NEOARM 200), and synchrotron-based X-ray absorption fine structure

spectroscopy (XAFS, including XANES and EXAFS). For the EXAFS analysis, the R-space spectra are not phase-corrected. Quantitative fitting was performed using the corresponding scattering paths.

Electrochemical Measurements: The freestanding Se/Co-NC@CNFs and Se/NC@CNFs films were punched into circular disks with a diameter of 8 mm and used directly as cathodes without any binder, current collector, or conductive additive. The Se/NC cathode was prepared by a conventional slurry-casting method, in which Se/NC, Super P, and poly(vinylidene fluoride) (PVDF) were mixed in a weight ratio of 7:2:1 in N-methyl-2-pyrrolidone (NMP) to form a uniform slurry. The slurry was coated onto aluminum foil, vacuum-dried at 60 °C overnight, and punched into circular disks with a diameter of 8 mm.

CR2032-type coin cells were assembled in an Ar-filled glove box (H_2O and O_2 < 0.1 ppm) using lithium foil as the anode and a Celgard 2300 membrane as the separator. The electrolyte was 1 M $LiPF_6$ in ethylene carbonate/diethyl carbonate/fluoroethylene carbonate (EC/DEC/FEC, 6:3:1 by volume). Unless otherwise specified, 150 μL electrolyte was used in each coin cell. For the Se/Co-NC@CNFs cathode in the main text, the Se areal loading was approximately 1.0 mg cm^{-2}. For the high-loading Se73/Co-NC@CNFs cathode, the Se areal loading was 1.75 mg cm^{-2}.

Cyclic voltammetry (CV) and electrochemical impedance spectroscopy (EIS) were carried out on a CHI660E electrochemical workstation. CV measurements were performed between 0.8 and 3.0 V (vs. Li^+/Li) at various scan rates. EIS was measured over a frequency range of 100 kHz to 10 mHz with an amplitude of 5 mV. Galvanostatic

charge/discharge tests were conducted on a LAND battery testing system within 0.8–3.0 V at room temperature. Soft-packaged batteries were also assembled with an electrode area of approximately 9 × 9.5 cm^2 and an electrolyte dosage of approximately 2.2 mL.

Capacitive contribution analysis: The capacitive contribution is calculated based on the following equations:

$$i = av^b \qquad \textbf{Eq. S1}$$

$$i(V) = k_1 v + k_2 v^{1/2} \qquad \textbf{Eq. S2}$$

Herein, $i(V)$ is the total current at a given potential V, v is the scan rate (V s^{-1}), a and b is the constant value. $k_1 v$ is the capacitive current (surface-controlled process, linearly proportional to scan rate); $k_2 v^{1/2}$ is the diffusion-controlled current (faradaic process, proportional to the square root of scan rate).

Li^+ diffusion coefficient (D_{Li}^+): The Li^+ diffusion coefficients (D_{Li}^+) is calculated based on the Fick's second law (Eq. S3), where L is the characteristic diffusion length, usually taken as the electrode thickness (cm), τ is the duration of the galvanostatic pulse (s), ΔE_s is the steady-state voltage change for the GITT step (V), ΔE_t is the voltage change during the pulse, after ohmic-drop correction (V).

$$D = \frac{4L^2}{\pi\tau}\left(\frac{\Delta E_s}{\Delta E_t}\right)^2 \qquad \textbf{Eq. S2}$$

2、 Figures and Tables

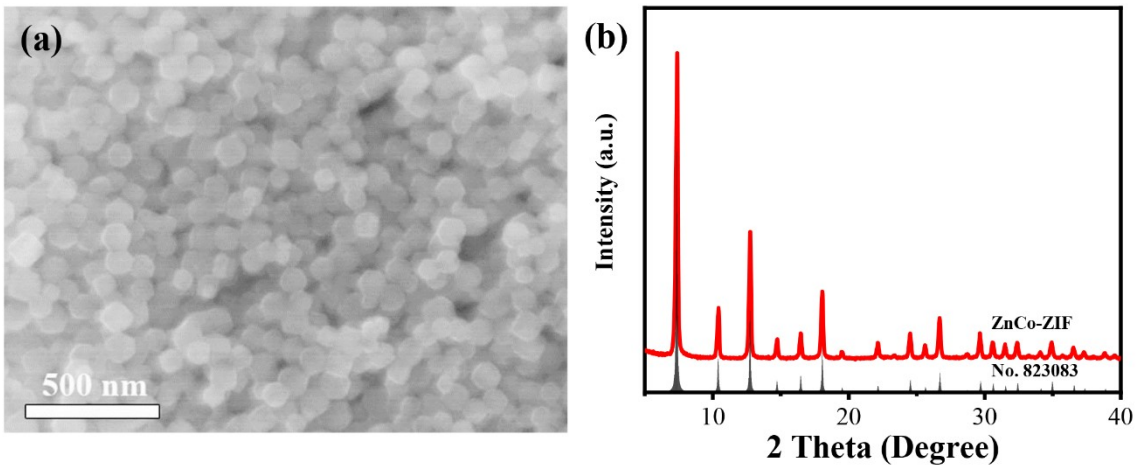

Fig. S1. (a) SEM image and (b) XRD pattern of ZnCo-ZIFs.

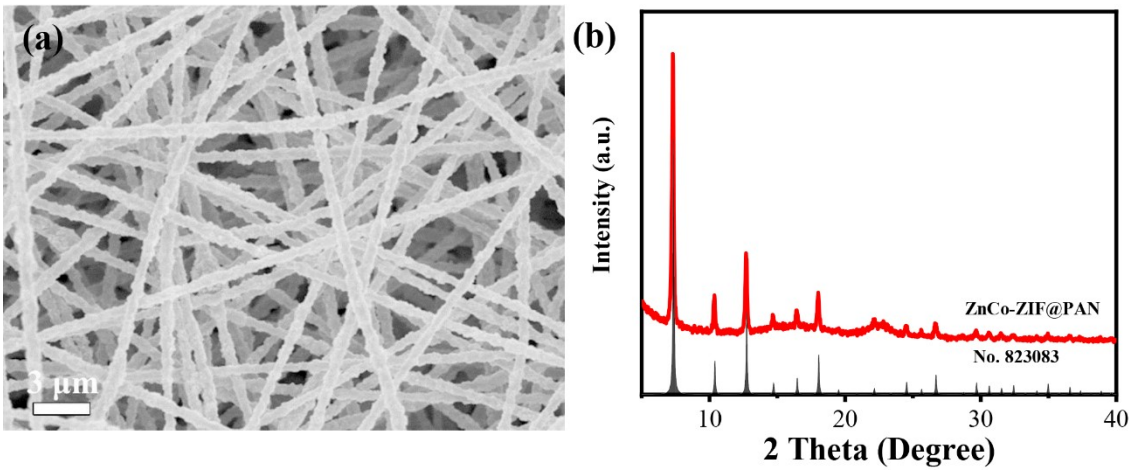

Fig. S2. (a) SEM image and (b) XRD pattern of the ZnCo-ZIFs@PAN.

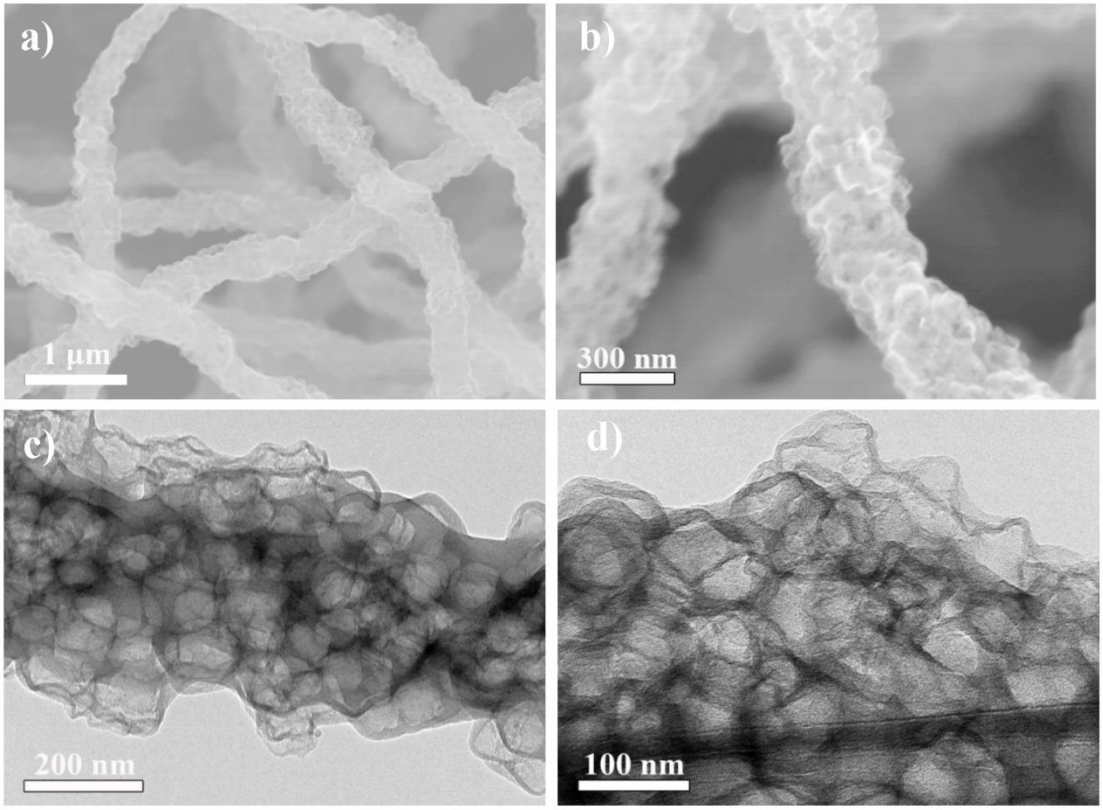

Fig. S3. (a, b) SEM images and (c, d) TEM images of the Co-NC@CNFs sample.

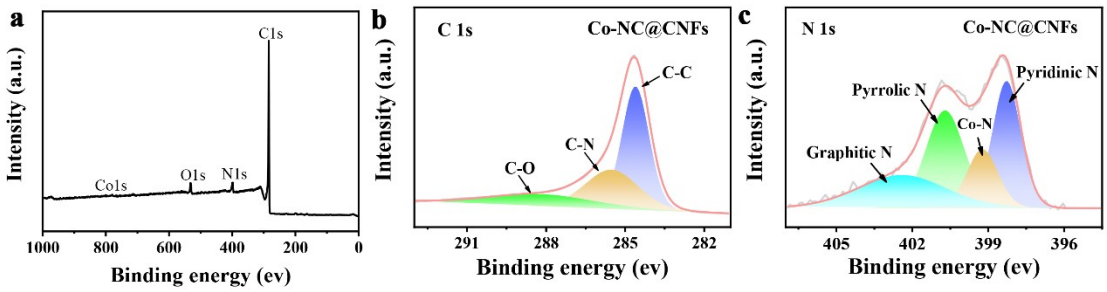

Fig. S4. (a) XPS survey and the corresponding high-resolution (b) C 1s, (c) N 1s spectrum of Co-NC@CNFs.

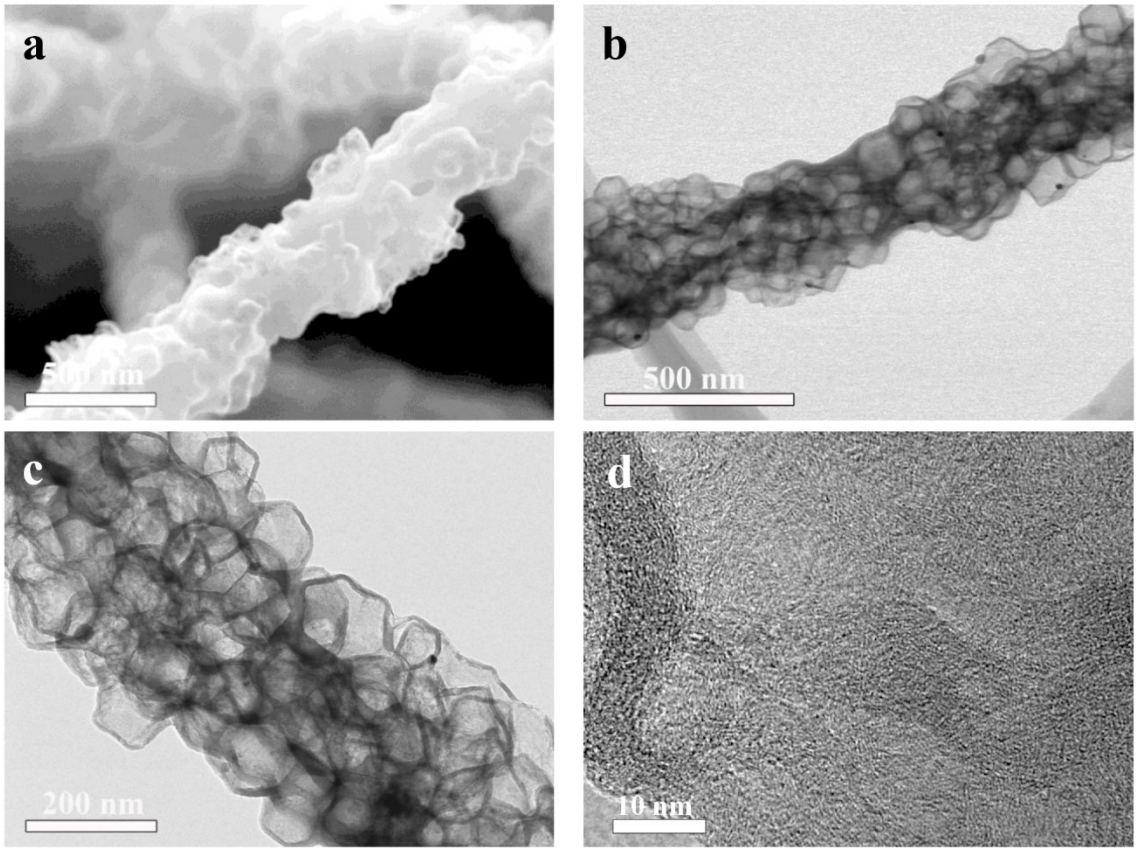

Fig. S5. (a) SEM image, (b, c) TEM images, and (d) HR-TEM image of Se/Co-NC@CNFs.

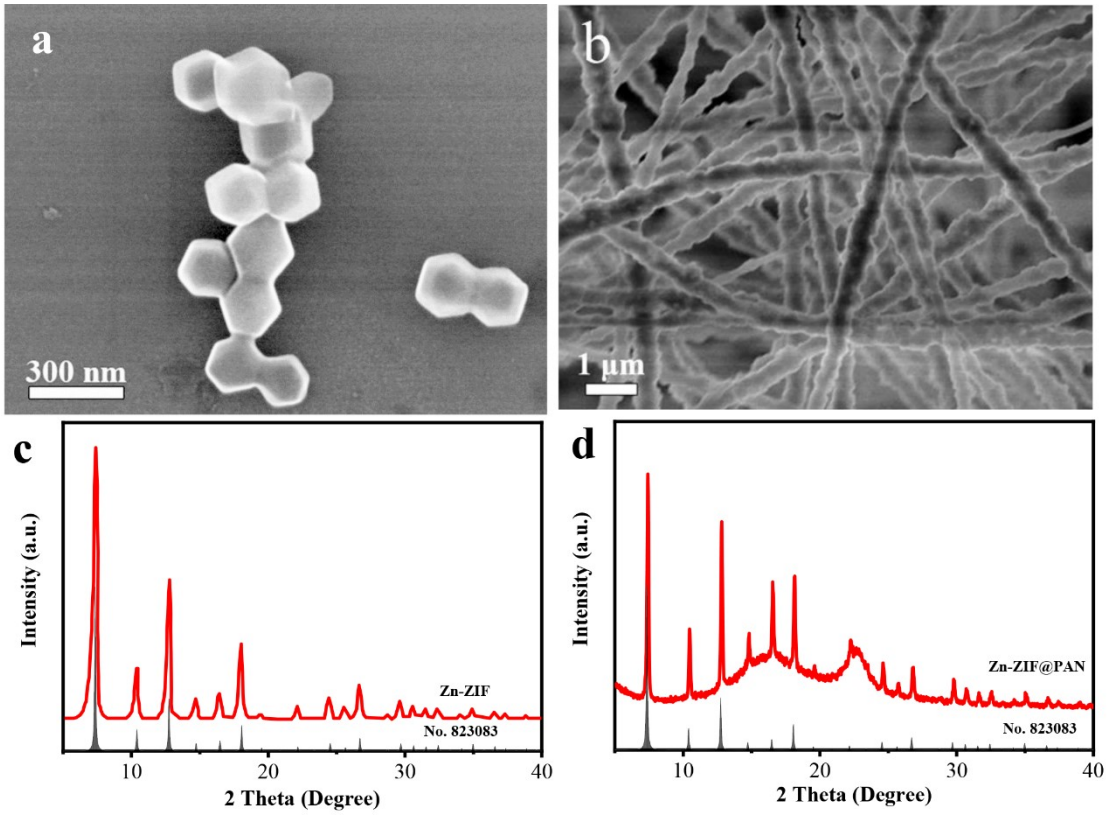

Fig. S6. (a, b) SEM images and (c, d) XRD patterns for the Zn-ZIF and Zn-ZIF@PAN, respectively.

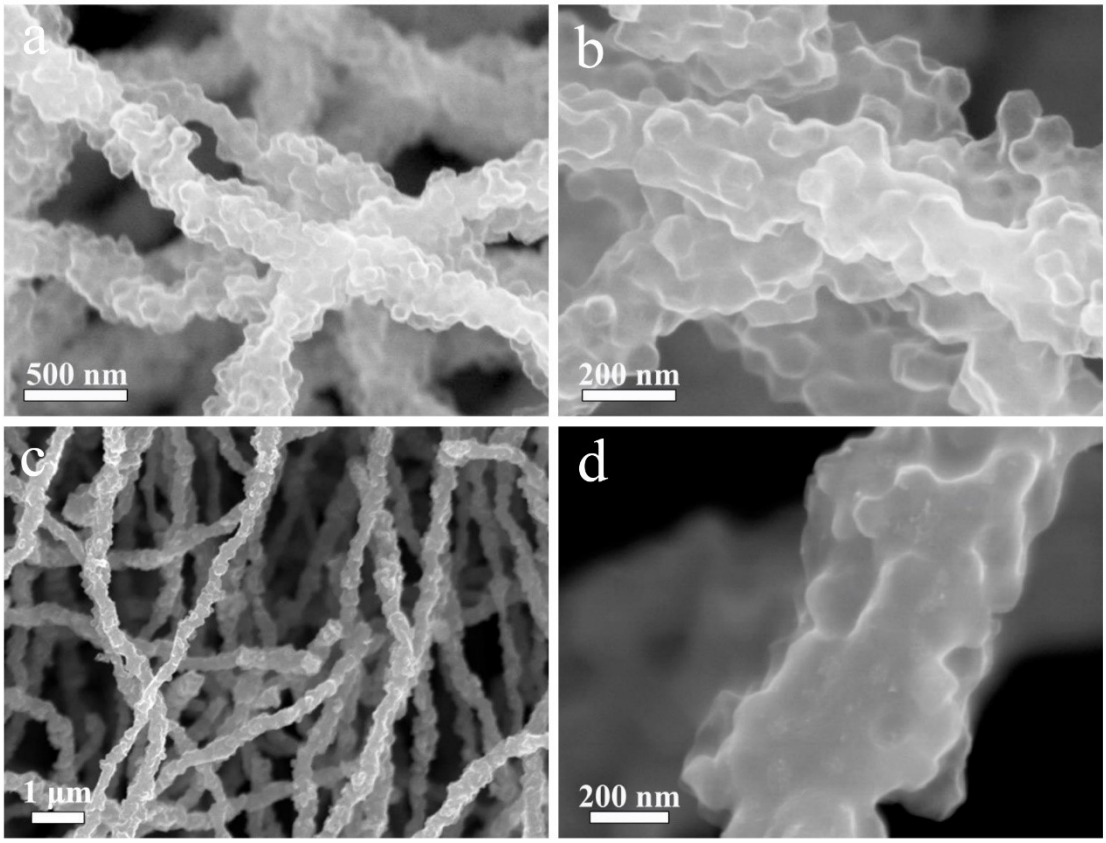

Fig. S7. (a, b) SEM images of the NC@CNFs. (c, d) SEM images of the Se/NC@CNFs.

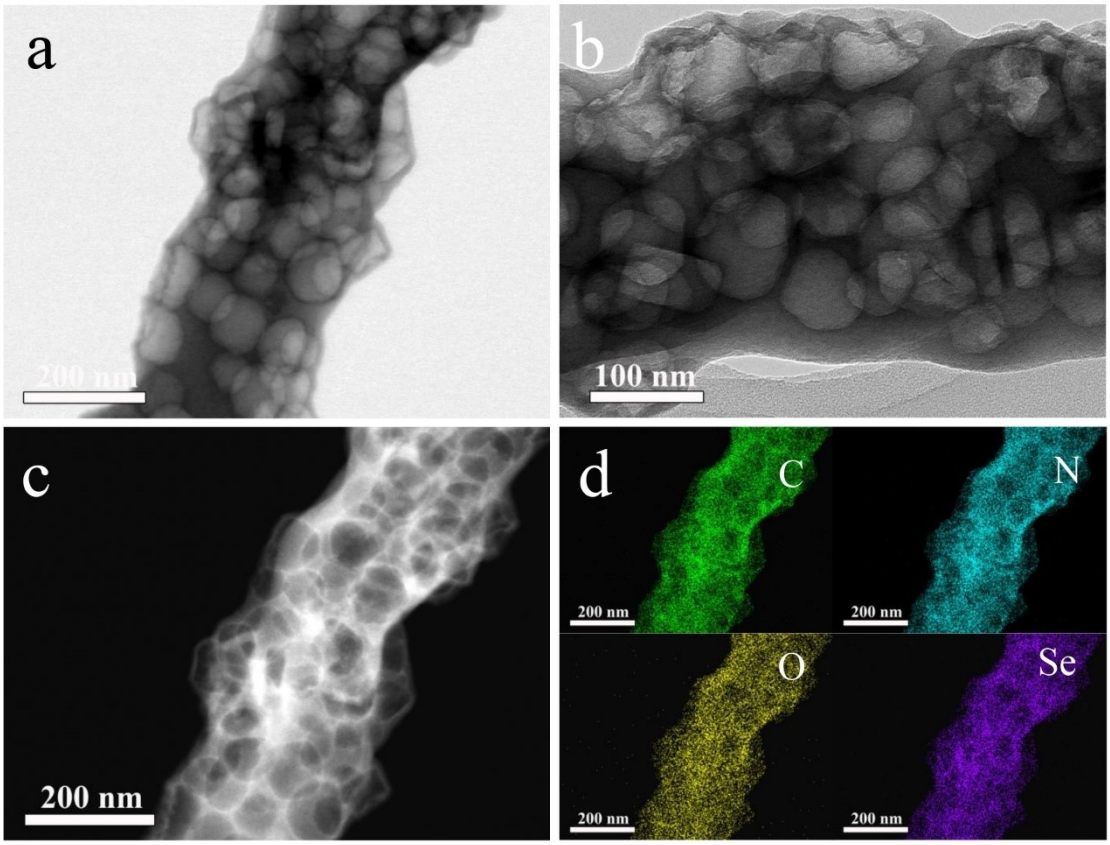

Fig. S8. (a, b) TEM images, (c) HAADF-STEM image, and (d) the corresponding element mappings of the Se/NC@CNFs.

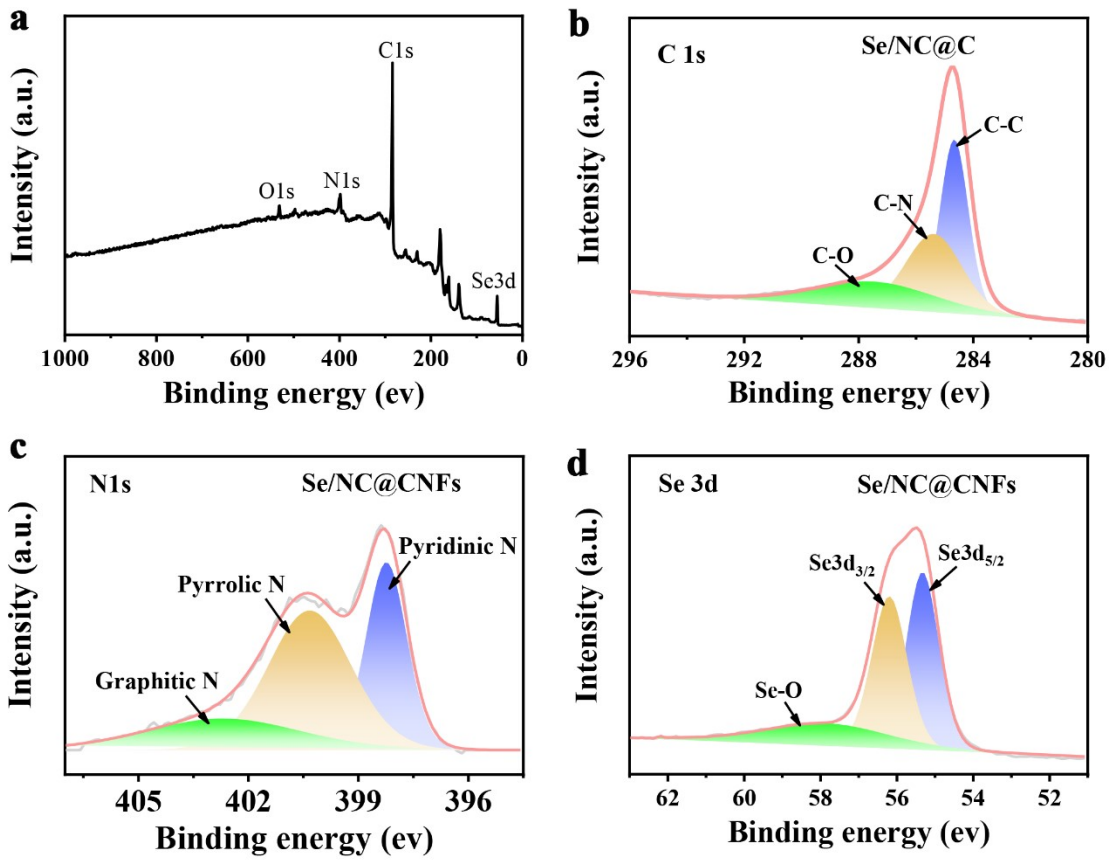

Fig. S9. (a) XPS survey spectrum and (b) High-resolution C 1s, (c) N 1s XPS spectrum, (d) Se 3d XPS spectrum of the Se/NC@CNFs.

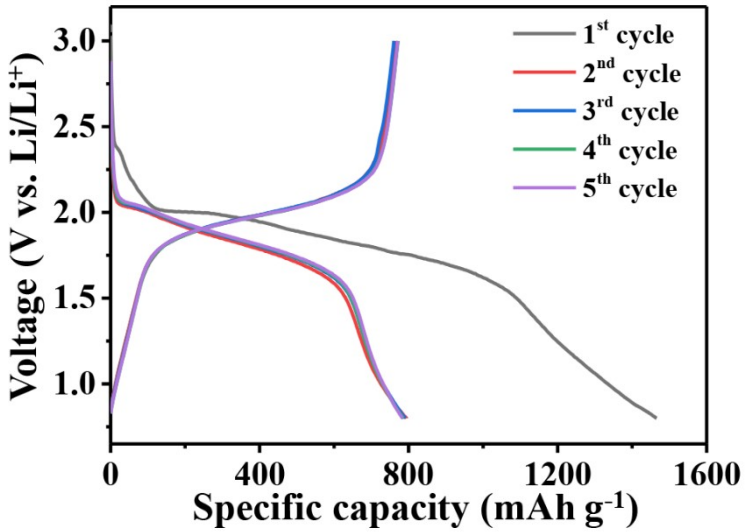

Fig. S10. Charge/discharge profiles of the Se/Co-NC@CNFs cathode

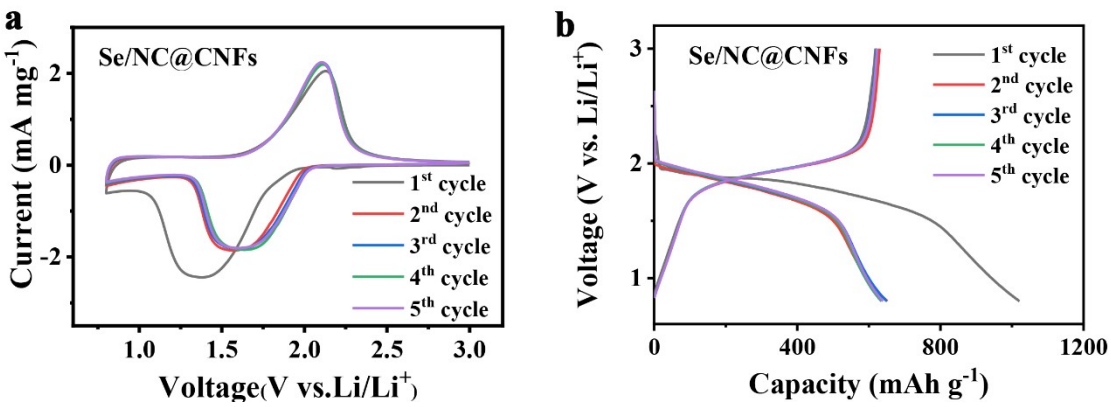

Fig. S11. (a) CV curves of Se/NC@CNFs cathode. (b) Galvanostatic charge/discharge curves of Se/NC@CNFs cathode at 0.1 A g^{-1}.

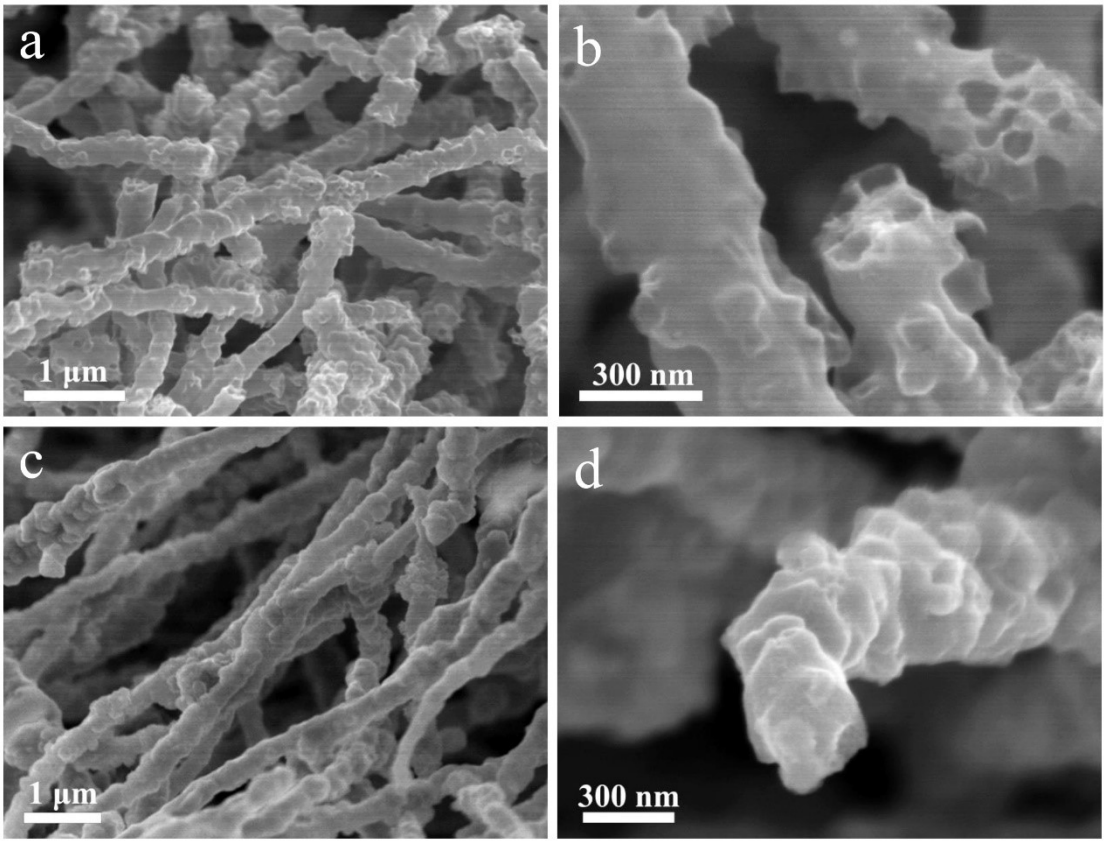

Fig. S12. SEM images of Se/Co-NC@CNFs cathode after 100 cycles in the discharged state.

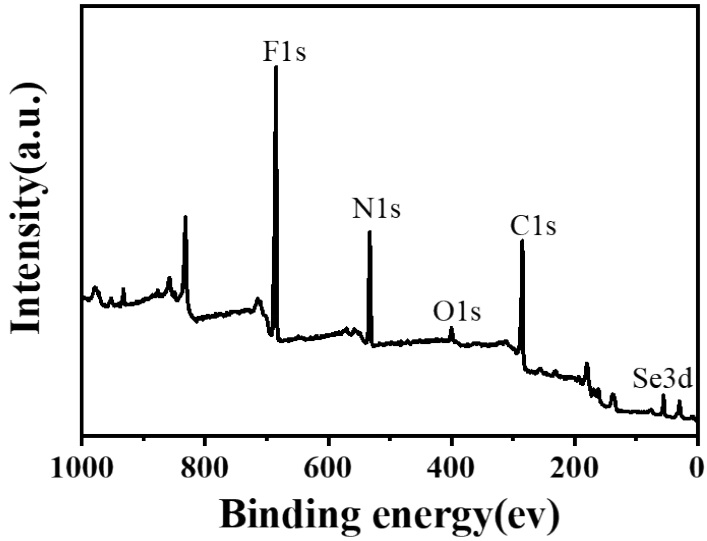

Fig. S13. XPS survey spectrum of Se/Co-NC@CNFs after cycling.

Table S1. ICP-OES results to determine the cobalt content in the Co-NC@CNFs.

Mass (g)	Volume (mL)	Element	C_0 (mgL^{-1})	Dilution factor	C_1 (mgL^{-1})	C_x ($mg\ kg^{-1}$)	Wt (%)
0.0572	100	Co	8.39	1	8.39	14667.83	1.467 %

Note: C_0: Element concentration in test solution; C_1: Element concentration in digest/original sample solution; C_x: Element content.

Table S2. Co *K*-edge EXAFS fitting parameters of Co-NC@CNFs samples.

Sample	Path	*CN*	*R* (Å)	σ^2 ($Å^2$)	ΔE_0 (eV)	*R*-factor
Co-NC@CNFs	Co-N	4.0 ± 0.5	1.95 ± 0.02	0.0035 ± 0.001	2.3 ± 1.5	1.5%

Note: CN is the coordination number; R is the interatomic distance between the absorber and backscattering atoms; σ^2 is the Debye–Waller factor accounting for thermal and structural disorder; ΔE_0 is the inner potential correction; and the R-factor estimates the goodness of fit.

Table S3. Electrochemical performance comparison with other representative cathodes in Li-Se batteries.

Cathodes	Se content (wt.%)	Cycling performance	Rate performance	Ref.
Se/Co-NC@CNFs	**50**	**15 A g^{-1}, 530 mAh g^{-1} (3500 cycles); 50 A g^{-1}, 500 mAh g^{-1} (2000 cycles)**	**50 A g^{-1} (~74 C), 545 mAh g^{-1}**	**This work**
FN@Se	50	1 A g^{-1}, 177 mAh g^{-1} (1000 cycles)	2 A g^{-1}, 163.4 mAh g^{-1}	S1
Se/OHPC	65	0.2 C, 380 mAh g^{-1} (200 cycles)	5 C, 150 mAh g^{-1}	S2
PNCNFs/Se@MXene	49.6	5 C, 298 mAh g^{-1} (3500 cycles)	20 C, 266 mAh g^{-1}	S3
SPC/Se	74.3	0.2 C, 587 mAh g^{-1} (1000 cycles)	20 C, 372 mAh g^{-1}	S4
APPC/Se@PDA	58	23 C, 274 mAh g^{-1} (2500 cycles)	5 C, 418 mAh g^{-1}	S5
Se@HHCS	45-48	5 C, 442 mAh g^{-1} (1500 cycles); 10 C, 357 mAh g^{-1}	10 C, 382 mAh g^{-1}	S6

		(2000 cycles)		
Se@Co $_{SA}$-HC	57	0.5 C, 457 mAh g^{-1} (1700 cycles); 50 C, 237 mAh g^{-1} (2500 cycles)	50 C, 311 mAh g^{-1}	S7
MiC/Se	44.2	0.5 C, 300 mAh g^{-1} (100 cycles)	5 C, 363 mAh g^{-1}	S8
Se@CISC-29	56.2	1 A g^{-1}, 590 mAh g^{-1} (500 cycles)	2 A g^{-1}, 507 mAh g^{-1}	S9
MPCS/Se	44.4	10 C, 400 mAh g^{-1} (1000 cycles)	10 C, 408 mAh g^{-1}	S10
Se@LHPC	52	0.5 C, 450 mAh g^{-1} (500 cycles)	2 C, 332 mAh g^{-1}	S11
CSe@HNCNFs	33	10 C, 465 mAh g^{-1} (1100 cycles)	50 C, 414 mAh g^{-1}	S12
Se@HMCS	55.7	0.05 A g^{-1}, 603.4 mAh g^{-1} (100 cycles)	3 A g^{-1}, 303 mAh g^{-1}	S13

3、 References:

[S1] K. Sun, X. Deng, X. Huang, S. Liao, L. Liu, M. Yang and T. Wei, Large-scale synthesis of N-doped carbon spherical shells as high-performance cathode materials for Li–X (X = O2, S, Se) batteries, **J. Mater. Chem. A**, 2024, **12**, 28863.

[S2] J. Li, J. Song, L. Luo, H. Zhang, J. Feng, X. Zhao, X. Guo, H. Dong, S. Chen, H. Liu, G. Shao, T. D. Anthopoulos, Y. Su, F. Wang and G. Wang, Synergy of MXene with Se infiltrated porous N-doped carbon nanofibers as Janus electrodes for high-performance sodium/lithium-selenium batteries, **Adv. Energy Mater.**, 2022, **12**, 2200894.

[S3] H. Li, W. Dong, C. Li, T. Barakat, M. Sun, Y. Wang, L. Wu, L. Wang, L. Xia, Z. Y. Hu, Y. Li and B. L. Su, Three-dimensional ordered hierarchically porous carbon materials for high performance Li–Se battery, **J. Energy Chem.**, 2022, **68**, 624.

[S4] Q. Zhao, Y. Meng, L. Su, W. Cen, Q. Wang and D. Xiao, Nitrogen/oxygen codoped hierarchical porous carbons/selenium cathode with excellent lithium and sodium storage behavior, **J. Colloid Interface Sci.**, 2022, **608**, 265.

[S5] Y. Cao, F. Lei, Y. Li, S. Qiu, Y. Wang, W. Zhang and Z. Zhang, A MOF-derived carbon host associated with Fe and Co single atoms for Li–Se batteries, **J. Mater. Chem. A**, 2021, **9**, 16196.

[S6] Y. Wang, H. Hao, S. Hwang, P. Liu, Y. Xu, J. A. Boscoboinik, D. Datta and D. Mitlin, Selenium infiltrated hierarchical hollow carbon spheres display rapid kinetics and extended cycling as lithium metal battery cathodes, **J. Mater. Chem. A**, 2021, **9**, 18582.

[S7] H. Tian, H. Tian, S. Wang, S. Chen, F. Zhang, L. Song, H. Liu, J. Liu and G. Wang, High-power lithium-selenium batteries enabled by atomic cobalt electrocatalyst in hollow carbon cathode, **Nat. Commun.**, 2020, **11**, 5025.

[S8] X. Wang, Y. Tan, Z. Liu, Y. Fan, M. Li, H. A. Younus, J. Duan, H. Deng and S. Zhang, New insight into the confinement effect of microporous carbon in Li/Se

battery chemistry: a cathode with enhanced conductivity, **Small**, 2020, **16**, 2000266.

[S9] Y. Lei, X. Liang, L. Yang, P. Jiang, Z. Lei, S. Wu and J. Feng, Novel hierarchical porous carbon prepared by a one-step template route for electric double layer capacitors and Li–Se battery devices, **J. Mater. Chem. A**, 2020, **8**, 4376

[S10] Z. Lei, Y. Lei, X. Liang, L. Yang and J. Feng, High stable rate cycling performances of microporous carbon spheres/selenium composite (MPCS/Se) cathode as lithium-selenium battery, **J. Power Sources**, 2020, **473**, 228611.

[S11] P. Lu, F. Liu, F. Zhou, J. Qin, H. Shi and Z.-S. Wu, Lignin derived hierarchical porous carbon with extremely suppressed polyselenide shuttling for high-capacity and long-cycle-life lithium-selenium batteries, **J. Energy Chem.**, 2021, **55**, 476

[S12] J. Zhou, M. Chen, T. Wang, S. Li, Q. Zhang, M. Zhang, H. Xu, J. Liu, J. Liang, J. Zhu and X. Duan, Covalent selenium embedded in hierarchical carbon nanofibers for ultra-high areal capacity Li–Se batteries, **iScience**, 2020, **23**, 100919.

[S13] P. Xue, Y. Zhai, N. Wang, Y. Zhang, Z. Lu, Y. Liu, Z. Bai, B. Han, G. Zou and S. Dou, Selenium@hollow mesoporous carbon composites for high-rate and long-cycling lithium/sodium-ion batteries, **Chem. Eng. J.**, 2020, **392**, 123676.